Original Research *Feature article*

LCZ696, an angiotensin receptor-neprilysin inhibitor, ameliorates diabetic cardiomyopathy by inhibiting inflammation, oxidative stress and apoptosis

Qing Ge*, Li Zhao*, Xiao-Min Ren, Peng Ye and Zuo-Ying Hu

Department of Cardiology, Nanjing First Hospital, Nanjing Medical University, Nanjing 210006, China
*These authors contributed equally to this paper.
Corresponding author: Zuo-Ying Hu. Email: huzuoying@aliyun.com

Impact statement

Diabetic cardiomyopathy (DCM) is an important cause of heart failure in patients with diabetes, resulting in increased morbidity and mortality. LCZ696, which was studied here, is a novel drug for the treatment of heart failure. The latest research reports that LCZ696 is more effective for preventing heart failure than valsartan alone. However, little research has been performed examining the effects of LCZ696 on DCM. This study was designed to examine the role played by LCZ696 during DCM and the potential mechanisms underlying these effects, which may provide the basis for a new therapeutic strategy for DCM.

Abstract

Diabetic cardiomyopathy, which refers to the destruction of the structure and function of the heart, is the primary cause of heart failure due to diabetes. LCZ696 is the first angiotensin receptor-neprilysin inhibitor (ARNi) to be used clinically. Our study investigated the role played by LCZ696 during diabetic cardiomyopathy and explored the potential mechanisms underlying these effects. Diabetes was induced by injecting streptozotocin intraperitoneally into mice, and the mice were then divided randomly into two groups: one group was treated with LCZ696 (60 mg/kg/d) for 16 weeks, and the other received no treatment. The H9C2 cardiomyoblast cell line was treated with LCZ696 under high-glucose (HG) conditions. The levels of apoptotic (Bax, Bcl-2 and cleaved caspase-3) and pro-inflammatory factors [nuclear factor (NF)-κB, c-Jun N-terminal kinase (JNK) and p38 mitogen-activated kinase (MAPK)] were assessed in heart tissues from diabetic and normal mice and in H9C2 cells. The heart tissue structures and cardiac functions of diabetic mice were compared with those of normal mice, using histological and echocardiographic analyses. The results showed that LCZ696 inhibits the nuclear transfer of NF-κB and JNK/p38MAPK phosphorylation, and mitigates inflammation and apoptosis in diabetic mice and H9C2 cardiomyocytes under HG conditions. The histological and echocardiographic data showed that compared with untreated diabetic mice, diabetic mice treated with LCZ696 exhibited improved ventricular remodeling and cardiac function. LCZ696 also ameliorated oxidative stress in both vivo and vitro. In conclusion, LCZ696 improved diabetic cardiomyopathy by reducing cardiac inflammation, oxidative stress, and apoptosis.

Keywords: LCZ696, diabetic cardiomyopathy, NF-κB, inflammation, oxidative stress, apoptosis

Experimental Biology and Medicine **2019; 244: 1028–1039. DOI: 10.1177/1535370219861283**

Introduction

Diabetic cardiomyopathy (DCM) is one of the most frequent and typical clinical features of diabetic cardiovascular complications and contributes to the impairment of both the function and the structure of the heart, increasing morbidity and mortality risks in diabetic patients.[1] Because of rapidly increasing prevalence and mortality of diabetes worldwide, examining the pathogenesis of DCM and identifying novel therapeutic adjuvants for the treatment of DCM is important.[2]

Evidence has demonstrated that the excessive cardiac inflammation, reactive oxygen species (ROS) generation, apoptosis, calcium ion regulation abnormalities, fatty acid metabolism abnormalities, and fibrotic reactions may play pivotal roles during the heart remodeling observed in DCM.[3,4] Among these, inflammation, oxidative stress,

and apoptosis appear to be the primary molecular mediators that underlie the pathogenesis of DCM. Inflammation and oxidative stress are crucial for the induction of apoptosis in cardiomyocytes via increased cytokine levels.[5] Interestingly, the activation of nuclear factor-κB (NF-κB) and mitogen-activated protein kinase (MAPK) pathways result in the increased expression of proinflammatory cytokines, which eventually contribute to heart failure and DCM.[5–8] Therefore, strategies that target inhibition of NF-κB and c-Jun N-terminal kinase (JNK)/p38MAPK may protect against inflammatory, oxidative stress, and apoptosis and could be effective for the treatment of DCM.

LCZ696, an angiotensin receptor-neprilysin inhibitor (ARNi), has been tested in clinical trials. LCZ696 is a combination of valsartan and AHU377, at a ratio of 1:1, which is synthesized through a complex chemical reaction, and it inhibits the excessive activation of the renin-angiotensin-aldosterone system (RAAS) while simultaneously increasing the cardiovascular protection provided by the natriuretic peptide system. Neprilysin inhibitors (NEPi) have been used as an adjunctive approach to the inhibition of the renin-angiotensin system (RAS), although the independent use of NEPis has failed in the market because their effectiveness has been determined to be unacceptably low.[9] LCZ696 has been reported to improve heart function effectively in streptozotocin (STZ)-induced diabetic mice and to reduce fibrosis by inhibiting transforming growth factor (TGF)-β during heart failure.[10] LCZ696 is considered to be one of the most important clinical breakthroughs in the field of cardiology over the past 10 years. LCZ696 was officially approved for clinical use by the US Food and Drug Administration (FDA) in July 2015, making it the first successfully marketed dual inhibitor of the angiotensin receptor and neprilysin; furthermore, it can significantly reduce heart failure, mortality, hospitalization, and other cardiovascular endpoints.[11–13] However, its therapeutic mechanism during DCM remains to be studied. Therefore, this study investigated the underlying mechanisms through which LCZ696 exerts anti-inflammatory, antioxidant, and antiapoptotic effects in an experimental model of DCM. In the present study, we used STZ-induced diabetic mice and high glucose (HG)-treated H9C2 cardiomyocytes to examine the effects of LCZ696 on cardiac inflammation, oxidative stress, and apoptosis and their associated signaling pathways. The results demonstrate that LCZ696 could potentially be used to treat DCM.

Materials and methods

Animal studies

All animal studies were performed in accordance with the Institutional Animal Care and Use Committee of Nanjing Medical University (Nanjing, China). Eight-week-old male C57BL/6 mice (19–23 g) were procured from the Animal Center of Nanjing Medical University. All mice were raised under standard environmental conditions (room temperature $23 \pm 2^{\circ}C$, humidity $55 \pm 5\%$, 12 h light/12 h dark cycle), with unrestricted access to food and water. To induce diabetes, mice were injected intraperitoneally with STZ (Sigma, St. Louis, MO, USA) for five consecutive days (55 mg/kg/d, dissolved in citrate buffer, pH 4.5). Seven days after the STZ injection, mice with blood glucose values ≥16.7 mmol/L were considered to be diabetic mice. Mice were divided randomly into the following four groups: (i) control group ($n = 10$); (ii) LCZ696 group ($n = 10$); (iii) diabetic mice (DM) group ($n = 15$); and (iv) DM + LCZ696 group ($n = 15$). LCZ696 and DM + LCZ696 mice were treated with LCZ696 (60 mg/kg/d, Novartis) for 16 weeks, and the corresponding control and diabetic groups were treated with saline. Blood glucose was measured from the tail vein 16 weeks after the administration of LCZ696. The cardiac functions of surviving mice were determined by using echocardiography after 16 weeks of treatment. After 16 weeks, the mice were euthanized, and their blood and hearts were collected for subsequent analyses.

Cell culture and intervention

H9C2 cells, acquired from the Shanghai Institute of Biochemistry and Cell Biology (Shanghai, China), were derived from rat hearts. H9C2 cells were cultured in Dulbecco's modified Eagle's medium (DMEM; Gibco, Rockville, MD, USA), containing 100 U/mL penicillin, 0.1 mg/mL streptomycin, 5.5 mmol/L D-glucose and 10% fetal bovine serum (FBS; Gibco). The Petri dish was placed in a humidified incubator containing 5% carbon dioxide at 37°C. As previously described,[6] cells were first cultured under normal glucose conditions (5.5 mM) with 3% FBS (the minimal essential medium) for 12 h, pretreated with LCZ696 (MCE) at concentrations of 1, 10, or 30 μM for 30 min, and then exposed to HG (33 mM) for 48 h.

Echocardiography

The cardiac structures and functions of the surviving mice were evaluated by the Vevo2100 system (Fujifilm Visual Sonics, Toronto, Canada), with a high-frequency (30 MHz) MS-400 transducer, at the Animal Center of Nanjing Medical University. The mice were anesthetized by the inhalation of isoflurane before the cardiac ultrasound was performed. The inducing dose of isoflurane was 3%, and the maintenance dose was 1.5% isoflurane. The cardiac function of the surviving mice was assessed by measuring the left ventricle internal dimension in systole (LVID,s) and diastole (LVID,d), the left-ventricular (LV) end volume in both diastole and systole, the left ventricular ejection fraction (LVEF), fraction shortening (FS) and the peak E/A ratio (E/A). The FS percentage (FS%) = [(LVID,d – LVID,s)/LVID,d] × 100. The LVEF percentage (EF%) = ([LV end-diastolic volume – LV end-systolic volume]/LV end-diastolic volume) × 100.

Physiological parameters and histopathological analysis

After measuring their body weights (BWs), the mice were euthanized, and the hearts were removed and weighed to obtain a heart weight (HW)/(BW) ratio. The tibia length

(TL) was also measured for each mouse, and the HW/TL ratio was used to indicate the nutritional status of each mouse. The heart tissue was fixed in 4% paraformaldehyde and then embedded in paraffin. The left ventricle was sliced into a 3–4-μm thick slices for hematoxylin-eosin (H-E) staining (Sigma), Sirius red staining (Sigma) and TUNEL staining (Roche, Indianapolis, IN, USA), according to the manufacturers' instructions. Pictures of stained tissues were obtained using a fluorescence microscope (original magnification ×400; Nikon, Tokyo, Japan).

Expression of inflammatory cytokines

The serum from each animal was separated from the blood sample, and the expression levels of the proinflammatory cytokines interleukin (IL)-1β, IL-6, TNF-β and N-terminal pro-B-type natriuretic protein (NT-proBNP) in the serum were detected using a corresponding enzyme-linked immunosorbent assay kit (ELISA; R&D Systems, Minnesota, MN, USA).

Biochemical test for liver and kidney function

Renal function was evaluated by serum creatinine and urea nitrogen levels, whereas hepatic function was assessed by aspartate transaminase and alanine aminotransferase levels. These indicators were determined using an Automatic Chemistry Analyzer (HITACHI 7100, Japan) in the Animal Core Facility of Nanjing Medical University.

The detection of glutathione (GSH) and the GSH/glutathione disulfide (GSSG) ratio

The levels of glutathione (GSH) and the GSH/glutathione disulfide (GSSG) ratios in mouse heart tissues were determined using the GSH and GSSG Assay Kit (Beyotime, Haimen, Jiangsu, China), according to the manufacturer's instructions.

Extraction of nuclear and cytoplasmic proteins

Cytoplasmic and nuclear proteins were extracted from mouse heart tissues and from H9C2 cells. All experimental procedures were performed using cytoplasmic and nuclear extraction kits (Thermo Fisher Scientific, Waltham, MA, USA), according to the manufacturer's instructions. The expression levels of NF-κB in both the cytoplasm and nucleus were detected by Western blotting.

Measurement of intracellular ROS production

The production of ROS in H9C2 cells was detected by dihydroethidium (DHE; Sigma) fluorescence. H9C2 cells were washed with 1×PBS after intervention, and then were incubated with DHE for 30 min at 37°C in the dark. Images were acquired using fluorescence microscopy.

Quantitative real-time polymerase chain reaction

Total RNA was extracted from cardiac tissue using TRIzol reagent (Invitrogen, Carlsbad, CA, USA). cDNA was produced using the PrimeScript RT reagent Kit (TakaRa Biotechnology, Dalian, China). Real-time PCR was performed with an ABI 7500 system (Grand Island, NY, USA), using the SYBR Premix Ex Taq kit (TakaRa Biotechnology). The reaction parameters were as follows: 95°C for 30 s for pre-denaturation, followed by 40 cycles of 95°C for 5 s and 60°C for 34 s. β-actin was used as a reference gene. All of the primers used are listed in Table 1.

Western blotting analysis

Lysis buffer, containing protease and phosphatase inhibitors, was added to left-ventricular tissue and H9C2 cells to extract proteins. The soluble protein concentrations were determined using a BCA protein assay (Thermo Fisher Scientific). Equal amounts of total extracted protein (20–80 μg) were separated by 10% or 12% gradient sodium dodecyl sulfate-polyacrylamide gel electrophoresis (SDS-PAGE) and transferred to polyvinylidene difluoride (PVDF) membranes. Nonspecific protein binding was blocked by incubating the membranes with blocking buffer (5% skimmed milk, 20 mM Tris HCl, pH 7.6, 150 mM NaCl, and 0.05% Tween-20) for 2 h at room temperature. Then, the membranes were incubated with specific primary antibodies against β-actin, Bax, Bcl-2, cleaved caspase-3, NF-κB, p-JNK, JNK, p-p38, p38, osteopontin (OPN), connective tissue growth factor (CTGF) (1:1000; Cell Signaling Technology Inc., Beverly, MA, USA), and histone (Santa Cruz Biotechnology Inc., Santa Cruz, CA, USA) in blocking buffer, with gentle shaking, overnight at 4°C. Subsequently, the membranes were washed three times for 15 min in Tris-buffered saline with Tween-20 (1×TBST). After incubation with a secondary antibody (1:1000; Cell Signaling Technology) for 2 h at room temperature, immunoreactive protein bands were visualized by chemiluminescence using a Syngene Bio Imaging Device (Syngene, Cambridge, UK). Densitometric analyses of immunoblots were performed using Image J software (National Institutes of Health, Bethesda, MD, USA).

Immunofluorescence staining

Immunofluorescence staining was performed as previously described.[14]

Table 1. Sequence of primers used for real-time polymerase chain reaction.

	5′-3′ (sense)	5′-3′ (antisense)
β-actin	CCAGATCATGTTTGAGACCT	TCTCTTGCTCGAAGTCTAGG
Collagen I	GCTCCTCTTAGGGGCCACT	ATTGGGGACCCTTAGGCCAT
Collagen III	CCTGGCTCAAATGGCTCAC	GACCTCGTGTTCCGGGTAT

Statistical analysis

Experimental data are expressed as the mean ± standard deviation (SD), and GraphPad Prism 6.01 software (La Jolla, CA, USA) was used to analyze these data. Statistical differences among groups were determined using a multiple-comparison one-way analysis of variance (ANOVA), with Bonferroni corrections. Values of $P < 0.05$ were considered to be significant.

Results

Sustained JNK/p38MAPK phosphorylation and NF-κB nuclear translocation are involved in HG-induced apoptosis in H9C2 cardiomyocytes

JNK, p38MAPK, and NF-κB are established pro-inflammatory factors that can induce cell apoptosis in diverse disease models, including heart failure and DCM.[5,15,16] Previous studies have demonstrated that persistent JNK/p38MAPK phosphorylation and NF-κB nuclear translocation occur in HG-treated neonatal rat ventricular cardiomyocytes.[7,8] To verify the effects of HG treatment on JNK/p38MAPK and NF-κB, H9C2 cardiomyocytes were stimulated with 33 mM HG for 4, 12, 24, or 48 h, and Western blotting was used to detect JNK/p38MAPK phosphorylation and NF-κB nuclear localization. As shown in Figure 1(a) and (b), longer stimulation with HG resulted in increased levels of phosphorylated JNK and p38MAPK and increased levels of NF-κB transported from the cytoplasm to the nucleus. Apoptosis markers, such as cleaved caspase-3 and the ratio of Bax to Bcl-2, increased significantly over time in H9C2 cells stimulated with HG (Figure 1(c)). These results suggest that HG stimulates JNK/p38MAPK phosphorylation and NF-κB nuclear translocation, which, in turn, promote apoptosis in H9C2 cardiomyocytes.

LCZ696 suppressed JNK/p38MAPK phosphorylation and NF-κB nuclear translocation in experimental models of DCM

To study the effects of LCZ696 on JNK/p38MAPK and NF-κB under conditions of HG stimulation, H9C2 cells were pretreated with LCZ696 at concentrations of 1, 10, or 30 μM for 30 min and then stimulated with HG for 48 h. As shown in Figure 2(a) to (d), HG- or diabetes-induced JNK/p38MAPK phosphorylation and NF-κB nuclear translocation were inhibited by the administration of LCZ696. NF-κB transport from the cytoplasm to the nucleus was significantly and increasingly attenuated with increasing LCZ696 concentrations, which was further confirmed by immunofluorescence (Figure 2(e)). These data indicated that LCZ696 inhibited the HG- or diabetes-induced JNK/p38MAPK phosphorylation and NF-κB nuclear translocation.

LCZ696 inhibited cell apoptosis in an experimental model of DCM

Apoptosis is an essential pathological process during the evolution of DCM. As shown in Figure 3(a) and (b), marked increases in the expression level of cleaved caspase-3 and in the ratio of Bax/Bcl-2 were observed in HG-treated H9C2 cells and diabetic hearts, and these increases could be inhibited by the administration of LCZ696, both *in vitro* and *in vivo*. Furthermore, and consistent with the above results, the number of TUNEL-positive cells in the heart tissues of diabetic mice was also significantly reduced by LCZ696 treatment (Figure 3(c) and (d)). These results demonstrated that LCZ696 inhibited HG- or diabetes-induced cell apoptosis.

LCZ696 inhibited oxidative stress and inflammation in an experimental model of DCM

A previous study has shown that the excessive production of ROS, stimulated by HG conditions, is an important factor during the evolution of DCM.[17] DHE staining was performed to determine whether LCZ696 inhibits HG-induced oxidative stress. DHE staining causes ROS in cells to exhibit red fluorescence. In normal cells, few cells had detectable levels of red fluorescence, suggesting low ROS levels. However, the intracellular ROS levels conspicuously increased after stimulation with 33 mM HG, whereas the administration of LCZ696 inhibited the HG-induced increase in ROS levels in a dose-dependent manner (Figure 4(a)). Moreover, decreased GSH contents and GSH/GSSG ratios were observed in diabetic mice, but these decreases were reversed by treatment with LCZ696 (Figure 4(b) and (c)). These data suggested that LCZ696 exerted anti-oxygenation effects in experimental models of DCM. Next, we investigated whether LCZ696 exerted anti-inflammatory effects in experimental models of DCM by detecting the expression levels of pro-inflammatory cytokines in mouse serum. As shown in Table 2, the expression levels of IL-1β, IL-6, and TNF-α in the serum of diabetic mice increased, but treatment with LCZ696 was able to reduce these levels. Additionally, the increase in the expression level of NT-proBNP in the serum of diabetic mice was also reduced by the administration of LCZ696. These results demonstrated that LCZ696 can also exert anti-inflammatory and anti-heart failure effects in an experimental model of DCM.

LCZ696 exerted anti-fibrotic effects in an experimental model of DCM

Increased inflammation and oxidative stress can cause collagen deposition, which leads to fibrosis. As shown in Figure 5(a) to (c), the protein expression levels of OPN and CTGF and the mRNA levels of collagen I and collagen III were higher in the heart tissue from diabetic mice than in the heart tissue from control mice, while these levels were lower in the groups that received LCZ696. Furthermore, we found that longer exposures to HG conditions resulted in larger increases in the protein levels of OPN and CTGF in H9C2 cells (Figure 5(d)). The increased protein expression levels of OPN and CTGF in HG-treated H9C2 cells could be reduced by the administration of LCZ696 in a concentration-dependent manner (Figure 5(e)). These data indicated that LCZ696 inhibited cardiac fibrosis in experimental models of DCM.

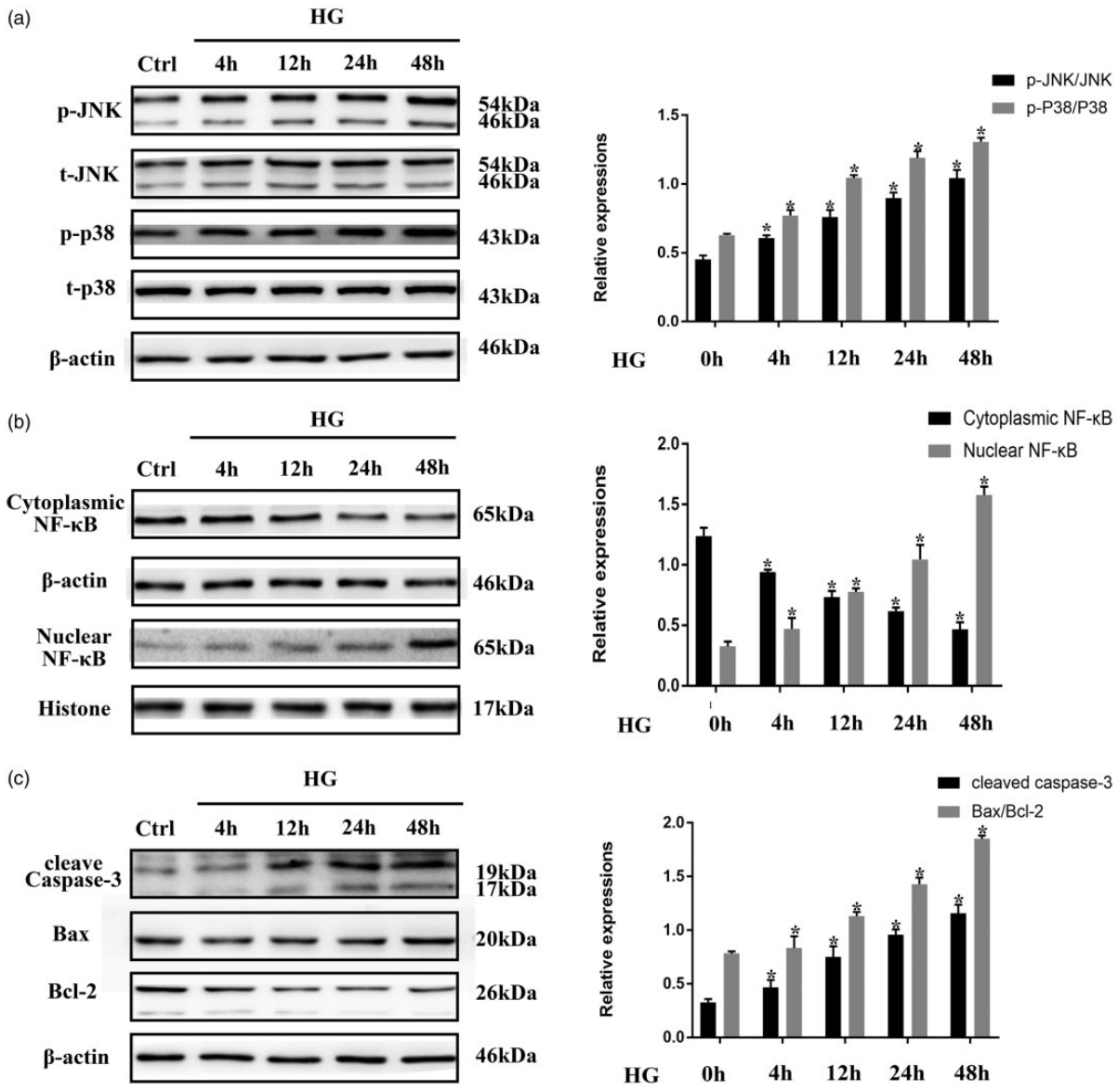

Figure 1. High glucose (HG) conditions induced the sustained activation of pro-inflammatory and apoptotic factors in H9C2 cells. (a) H9C2 cells were exposed to HG conditions for the indicated time periods. Phosphorylation of JNK and p38MAPK and total concentrations of JNK and p38MAPK were determined by Western blotting. (b) and (c) After the same treatment procedures described for (a), the nuclear translocation of NF-κB, the protein expression level of cleaved caspase-3, and the Bax/Bcl-2 ratio were determined using Western blotting. All data represent the average of three independent experiments and are expressed as the mean $\pm$ SD. $^*P < 0.05$ vs. Control.

LCZ696 inhibited cardiac remodeling and improved cardiac dysfunction in diabetic mice

We stained mouse heart tissue sections to examine changes in the heart structures in diabetic mice and to determine whether LCZ696 has any effect on these structures. As shown in Figure 6(a) and (b), H-E and Sirius red staining revealed structural disorder and increased levels of collagen fibers in diabetic mouse cardiomyocytes, and these abnormal pathological changes were partially improved by treatment with LCZ696. Transthoracic echocardiography was also performed to investigate whether LCZ696 could improve the cardiac dysfunction associated with DCM. We found that the left ventricular contraction and diastolic functions of diabetic mice were severely impaired, but this impairment was relieved in diabetic mice treated with LCZ696 for 16 weeks (Figure 6(c) and Supplementary Table 1). HW, BW, TL of mice were also measured, and the data are shown in Table 3. Diabetic mice had lower BW, HW, and HW/TL values but had higher HW/BW values than the control group, and these changes were ameliorated by the administration of LCZ696. Furthermore, LCZ696 treatment relieved diabetes-induced abnormal renal dysfunction without affecting liver function (Supplementary Table 2).

Discussion

In this study, HG treatment and diabetes induction generated oxidative stress and increased the expression levels of pro-inflammatory cytokines and pro-apoptotic factors. These effects were significantly attenuated by the

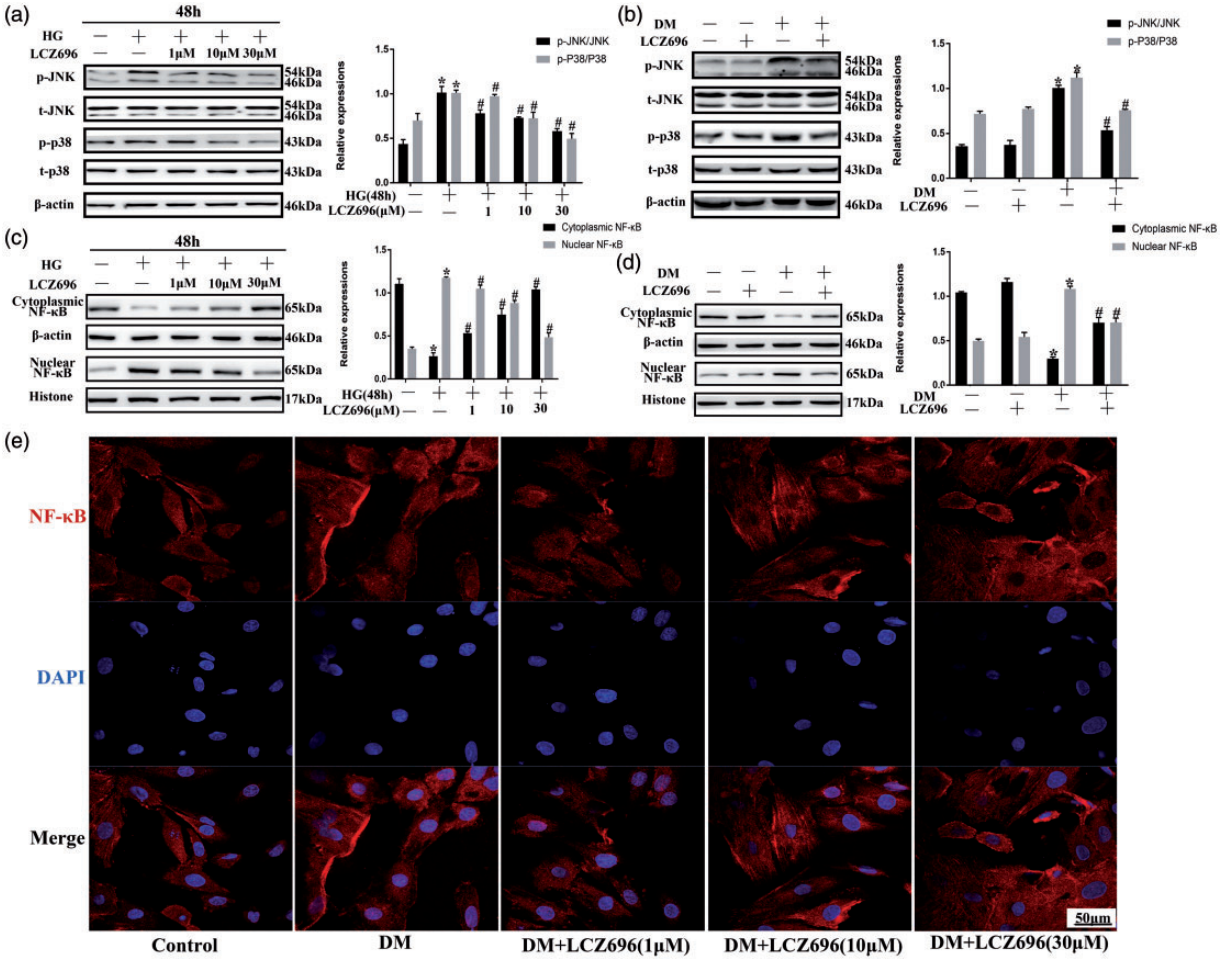

Figure 2. LCZ696 inhibited JNK and p38MAPK phosphorylation and NF-κB nuclear translocation in experimental models of DCM. (a) H9C2 cells were pretreated with or without LCZ696 at the indicated concentrations for 0.5 h and then exposed to HG conditions for 48 h. Phosphorylation of JNK and p38MAPK and total concentrations of JNK and p38MAPK were determined by Western blotting. (b) Mice treated with or without LCZ696 at the indicated dose were evaluated for JNK and p38MAPK phosphorylation and the total concentrations of JNK and p38MAPK were determined by Western blotting. (c) and (d) After the same treatment procedures described for (a) and (b), the nuclear translocation of NF-κB were determined using Western blotting. (e) Following the treatment described in (a) the nuclear translocation of NF-κB (in red) was determined using an immunofluorescence assay. Nuclei were stained with DAPI (in blue). Scale bar = 50 μm. Data in (a), (c) and (e) were obtained from at least three independent experiments. Data in (b) and (d) were obtained from four mice in each group. All data are expressed as the mean ± SD. $^{*}P < 0.05$ vs. Control; $^{\#}P < 0.05$ vs. HG or DM. (A color version of this figure is available in the online journal.)

administration of LCZ696. Furthermore, cardiac remodeling and cardiac dysfunction were also observed to improve in diabetic mice treated with LCZ696. Therefore, identifying the mechanisms that underlie these cardio-protective effects of LCZ696 has important clinical value.

Several studies have demonstrated that oxidative stress and inflammation can induce apoptosis and lead to the loss of contractile cardiomyocytes, ventricular remodeling, and eventual heart failure, all of which play pivotal roles in the pathogenesis of DCM.[5,6,17] The phosphorylation of JNK and p38MAPK and the nuclear translocation of NF-κB are also involved in the progression of heart failure.[15,16,18] Interestingly, increased levels of JNK and p38MAPK phosphorylation and increased NF-κB nuclear translocation have also been observed in DCM,[5–8] which is characterized by diastolic and/or systolic myocardial dysfunction.[8] Furthermore, a body of studies has indicated that JNK and p38MAPK, along with NF-κB, can initiate inflammation and oxidative stress, leading to apoptosis in diverse disease models.[19–21] In this study, sustained JNK/p38MAPK phosphorylation and NF-κB nuclear translocation, along with increased levels of pro-inflammatory cytokines, ROS and apoptotic factors, were observed in experimental models of DCM. These findings are consistent with those reported by previous studies.[5–8] Thus, targeting the inhibition of JNK and p38MAPK phosphorylation or NF-κB nuclear translocation could result in protection against inflammation, oxidative stress, and apoptosis and may represent an effective treatment option for DCM.

LCZ696, an ARNi, is a composite preparation composed of the angiotensin II receptor blocker valsartan and the NEPi sacubitril.[22] According to previous reports, LCZ696 demonstrates superior antihypertensive, anti-atherosclerotic, and cardiovascular and renal protective effects in diabetic animal models than angiotensin-converting enzyme inhibitor drugs.[9,23] Suematsu *et al.*[23] showed that LCZ696 treatment suppressed the activation of NF-κB, which in turn inhibited the expression of its

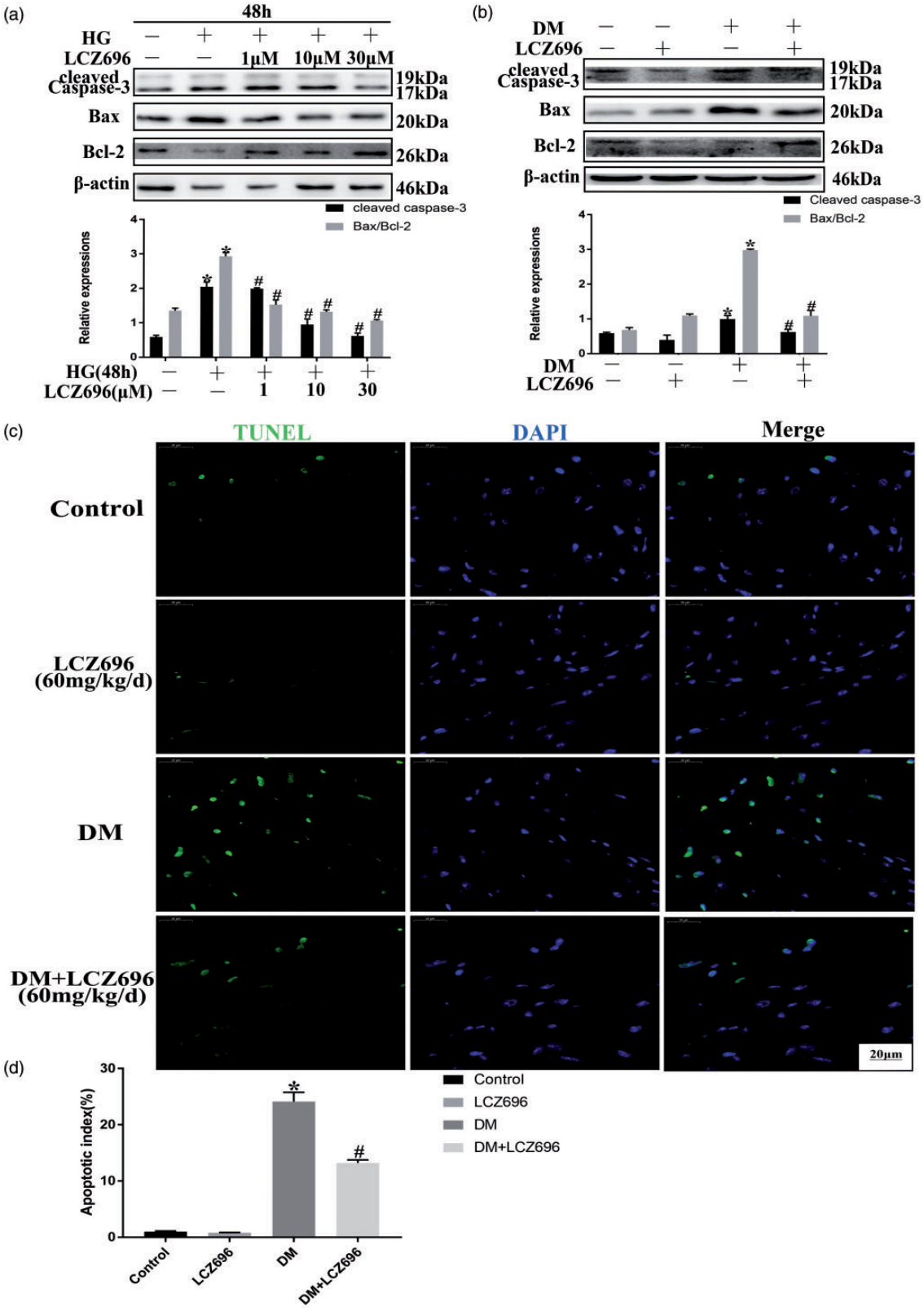

Figure 3. LCZ696 inhibited apoptosis in experimental models of DCM. (a) H9C2 cells were pretreated with or without LCZ696 at the indicated concentrations for 0.5 h and then exposed to HG conditions for 48 h. The protein expression level of cleaved caspase-3 and the Bax/Bcl-2 ratio was determined using Western blotting. (b) Mice treated with or without LCZ696 at the indicated dose were evaluated for the protein expression level of cleaved caspase-3 and the Bax/Bcl-2 ratio using Western blotting. (c) TUNEL-positive cells were examined in mice treated with or without LCZ696 at the indicated dose. Scale bar = 20 μm. (d) Quantification of the percentage of apoptotic TUNEL-positive cells. Data in (a) were obtained from at least three independent experiments. Data in (b) and (c) were obtained from 4 mice in each group. All data are expressed as the mean ± SD. $^{*}P < 0.05$ vs. Control; $^{\#}P < 0.05$ vs. HG or DM. (A color version of this figure is available in the online journal.)

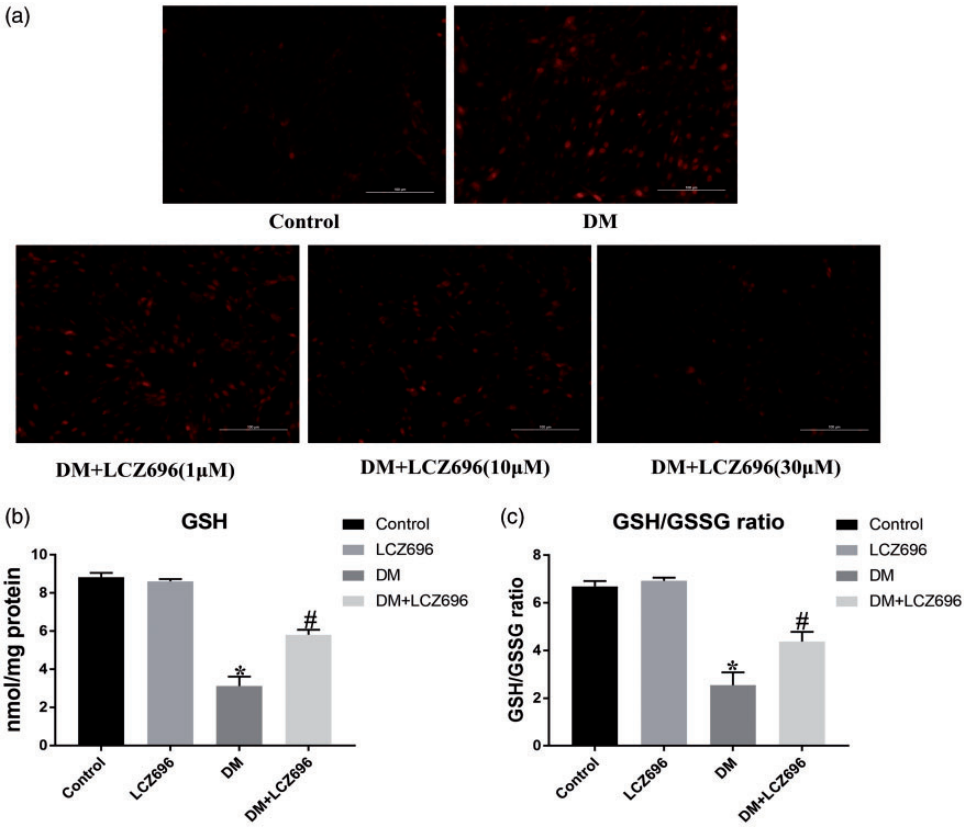

Figure 4. LCZ696 inhibited oxidative stress in experimental models of DCM. (a) H9C2 cells were pretreated with or without LCZ696 at the indicated concentrations for 0.5 h and then exposed to HG conditions for 48 h. Production of ROS was determined by DHE staining. Scale bars = 100 μm. (b) and (c) The level of GSH and the GSH/GSSG ratio was determined in mice with or without LCZ696 treatment at the indicated dose. Data in (a) were obtained from at least three independent experiments. Data in (b) and (c) were obtained from six mice in each group. All data are expressed as the mean ± SD. *$P < 0.05$ vs. Control; #$P < 0.05$ vs. DM. (A color version of this figure is available in the online journal.)

Table 2. Inflammatory cytokines production of mouse serum for 16 weeks.

Parameters	Control	Control + LCZ696 (60 mg/kg/d)	DM	DM + LCZ696 (60 mg/kg/d)
TNF-α (pg/mL)	6.262 ± 0.280	6.083 ± 0.327	8.006 ± 0.845*	6.759 ± 0.795#
IL-6 (pg/mL)	3.783 ± 0.800	3.259 ± 0.641	5.309 ± 0.866*	3.899 ± 0.472#
IL-1β (pg/mL)	3.232 ± 0.530	3.127 ± 0.458	4.966 ± 0.865*	3.416 ± 1.139#
NT-proBNP (ng/mL)	0.027 ± 0.010	0.021 ± 0.013	0.053 ± 0.021*	0.031 ± 0.015#

Note: Control, $n = 10$; Control+ LCZ696, $n = 10$; DM, $n = 10$; DM+ LCZ696, $n = 12$.
Data shown are the mean ± SD. *$P < 0.05$ vs. Control; #$P < 0.05$ vs. DM.

downstream molecules, such as monocyte chemoattractant protein 1 (MCP-1) and NADP oxidase-4, preventing the cardiovascular dysfunction caused by chronic kidney disease. In this study, LCZ696 significantly inhibited the persistent phosphorylation of JNK and p38MAPK and the nuclear translocation of NF-κB, resulting in anti-inflammatory, anti-oxygenation, anti-apoptotic, and cardioprotective effects in experimental models of DCM. Additionally, the administration of LCZ696, at a dose of 60 mg/kg/d, improved renal dysfunction and the survival rate of diabetic mice (Supplementary Figure 1), which could be attributed to the effects mentioned above. These findings suggest that LCZ696 may be an ideal therapeutic drug for DCM. However, the potential molecular mechanism through which LCZ696 negatively regulates JNK, p38MAPK, and NF-κB during DCM remains unclear. Previous studies have reported that TGF-β-activated kinase (TAK1) and MAPK kinase 4 (MKK4), which are upstream of JNK and p38MAPK,[24] and IκB kinase (IKK) and IκBα, which are upstream of NF-κB, are also involved in heart failure.[18] Whether LCZ696 has direct effects on the TAK1/MKK4-JNK/p38MAPK or IKK/IκBα-NF-κB pathways or whether it effects downstream molecules, such as MCP-1, remains to be studied. Although our study showed that LCZ696 improved DCM through its anti-inflammatory, anti-oxygenation, and anti-apoptotic effects, the effects of the enhanced natriuretic peptide system on these pathways and the identifying the specific mechanisms of action

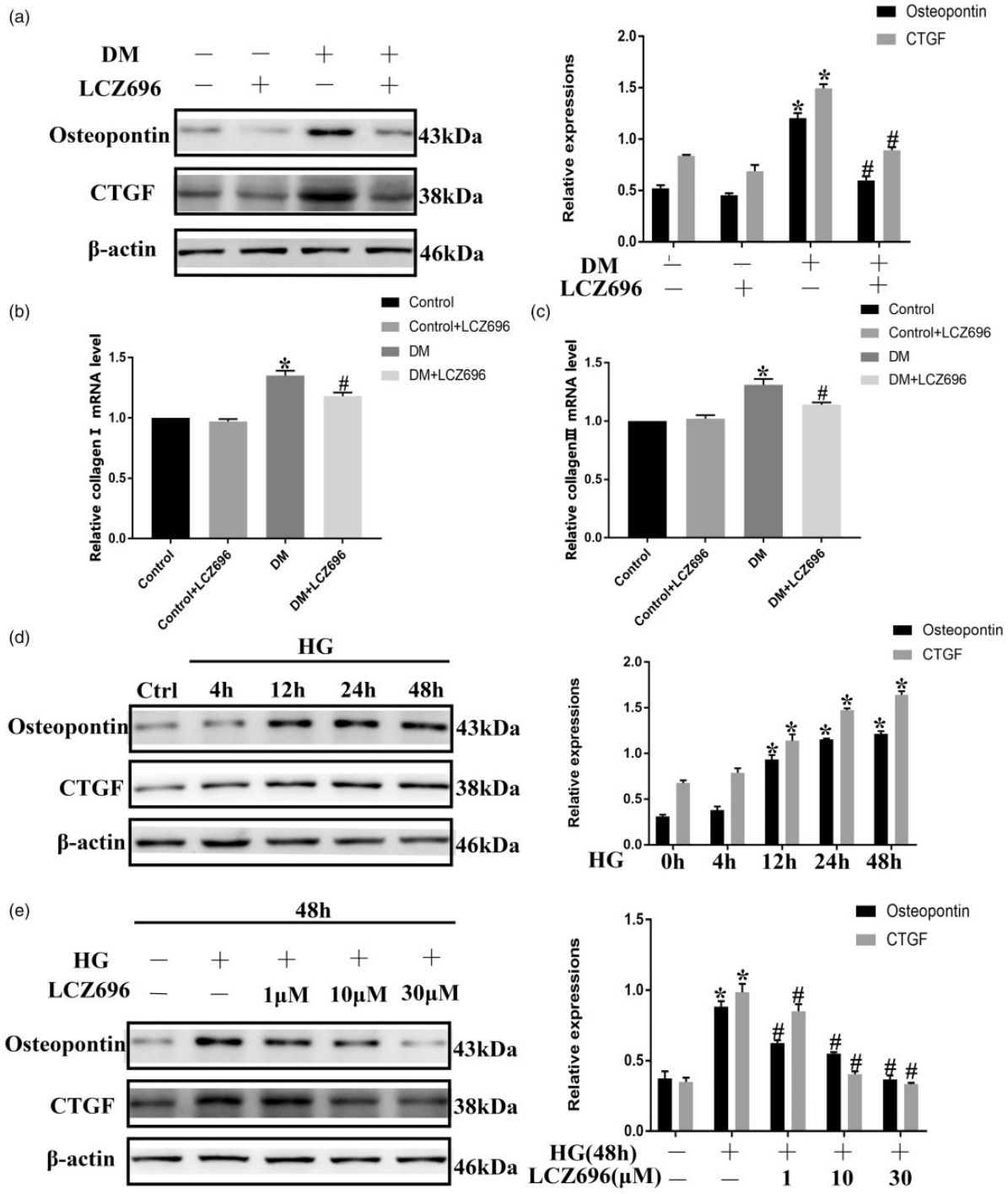

Figure 5. LCZ696 inhibited fibrosis in H9C2 cells cultured under HG conditions and in diabetic mice. (a) Mice treated with or without LCZ696 at the indicated dose were evaluated for the protein expression levels of OPN and CTGF by Western blotting. (b) and (c) After the same treatment procedures described for (a), the mRNA expression levels of collagen I and collagen III were evaluated by RT-PCR. (d) H9C2 cells were exposed to HG conditions for the indicated time periods. The protein expression levels of OPN and CTGF were determined by Western blotting. (e) H9C2 cells were pretreated with or without LCZ696 at the indicated concentrations for 0.5 h and then exposed to HG conditions for 48 h. The protein expression levels of OPN and CTGF were determined by Western blotting. Data in (a)–(c) were obtained from four mice in each group. Data in (d) and (e) were obtained from at least three independent experiments. All data are expressed as the mean ± SD. $^{*}P < 0.05$ vs. Control; $^{\#}P < 0.05$ vs. HG or DM.

require further research. Furthermore, neprilysin enzymes can degrade not only natriuretic peptides but also other vasoactive peptides. Whether LCZ696 can increase the expression levels of these vasoactive peptides still remains to be studied.

Our study showed that LCZ696 can protect against DCM by inhibiting inflammation, oxidative stress, and apoptosis (Supplementary Figure 2) without toxic effects. Therefore, LCZ696 might represent a potential new drug for the treatment of DCM.

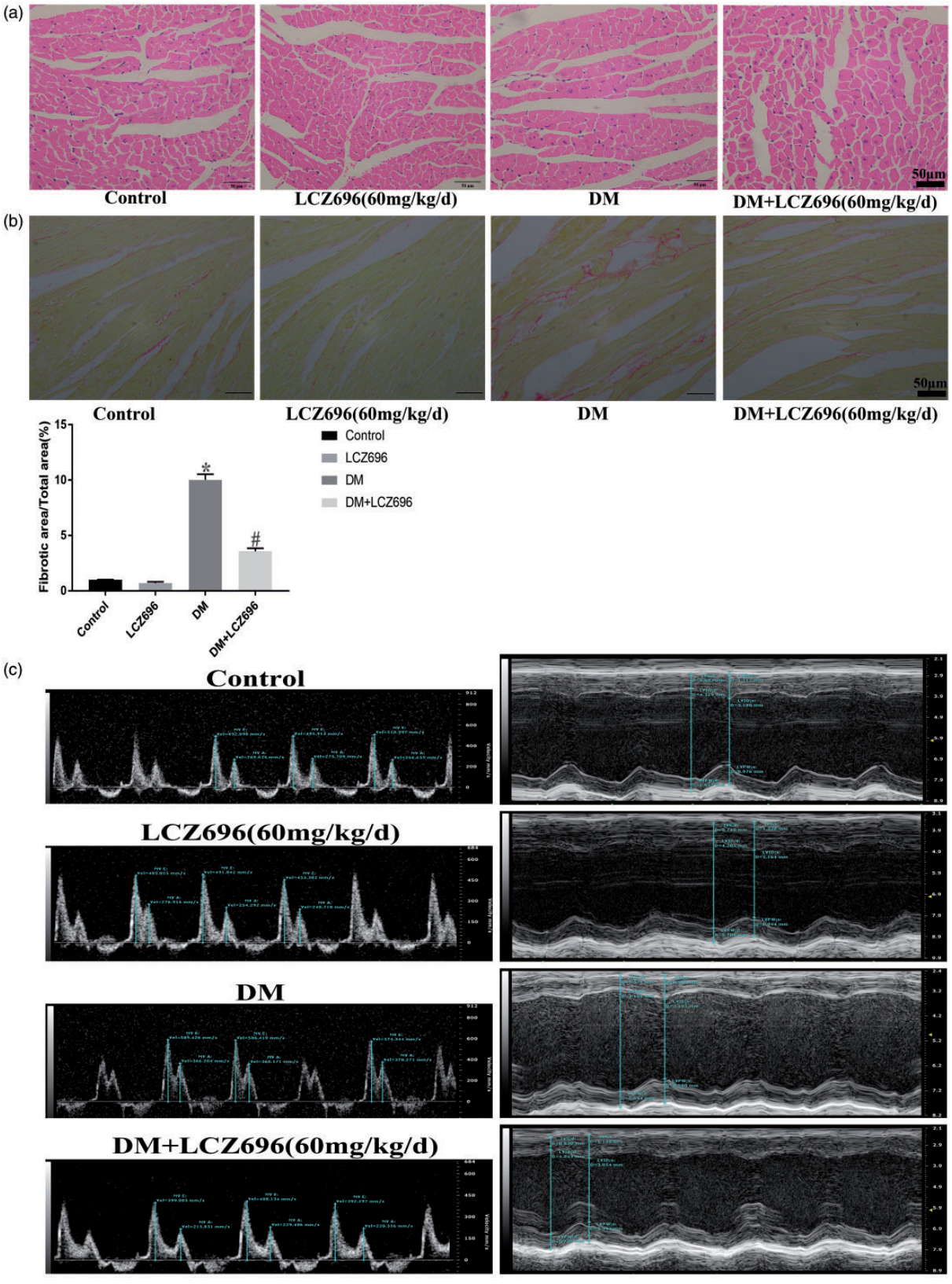

Figure 6. LCZ696 inhibited histological alterations and improved cardiac dysfunction in diabetic mice. H-E staining (a), Sirius red staining (b) and representative M-mode echocardiograms (c) were performed in mice treated with or without LCZ696 at the indicated dose. Scale bars = 50 μm. E, Peak velocity of the early ventricular filling (E wave); A, peak velocity of the late ventricular filling (A wave). Data in (a)–(c) were obtained from six mice in each group. All data are expressed as the mean ± SD. The column figure shows the differences in Sirius red staining. $^{*}P < 0.05$ vs. Control; $^{\#}P < 0.05$ vs. DM. (A color version of this figure is available in the online journal.)

Table 3. Physiological parameters of experimental mice at 16 weeks.

Parameters	Control	Control+LCZ696 (60 mg/kg/d)	DM	DM+LCZ696 (60 mg/kg/d)
Body weight (g)	33.63±1.309	32.11±0.842	25.56±1.066*	28.13±0.509#
Heart weight (mg)	135.3±2.530	134.2±2.197	109.1±3.376*	120.4±2.058#
Heart/body weight ratio (mg/g)	3.875±0.145	3.893±0.076	4.338±0.060*	3.998±0.083#
Tibial length (mm)	18.89±0.351	19.12±0.527	19.06±0.448	18.82±0.288
Heart weight/Tibial length (mg/mm)	6.963±0.182	6.847±0.203	5.777±0.292*	6.534±0.173#

Note: Control, $n = 10$; Control+ LCZ696, $n = 10$; DM, $n = 10$; DM+ LCZ696, $n = 12$.
Data shown are the mean ± SD. *$P < 0.05$ vs. Control; #$P < 0.05$ vs. DM.

Authors' contributions: All authors participated in the design and interpretation of the studies, the analysis of the data, and the review of the manuscript. QG, LZ, and XMR conducted the experiments and collected the data, QG and PY were responsible for the analysis and mapping of the data. PY provided methodological and technical guidance. QG wrote the manuscript, and ZYH reviewed the manuscript. All authors read and approved the final manuscript.

ACKNOWLEDGEMENTS

We thank Guang-Feng Zuo and Shao-Liang Chen for their technical assistance. We thank Lisa Giles, PhD, from Liwen Bianji, Edanz Editing China (www.liwenbianji.cn/ac), for editing the English text of a draft of this manuscript.

DECLARATION OF CONFLICTING INTERESTS

The author(s) declared no potential conflicts of interest with respect to the research, authorship, and/or publication of this article.

FUNDING

The author(s) disclosed receipt of the following financial support for the research, authorship, and/or publication of this article: This work was supported by the Key Project, under the Medical Science and Technology Development Foundation, Nanjing Department of Health (AKX18032).

ORCID iD

Qing Ge https://orcid.org/0000-0001-7377-9666

REFERENCES

1. Garcia MJ, McNamara PM, Gordon T, Kannel WB. Morbidity and mortality in diabetics in the Framingham population. Sixteen year follow-up study. *Diabetes* 1974;**23**:105–11
2. Danaei G, Finucane MM, Lu Y, Singh GM, Cowan MJ, Paciorek CJ, Lin JK, Farzadfar F, Khang YH, Stevens GA, Rao M, Ali MK, Riley LM, Robinson CA, Ezzati M. National, regional, and global trends in fasting plasma glucose and diabetes prevalence since 1980: systematic analysis of health examination surveys and epidemiological studies with 370 country-years and 2.7 million participants. *Lancet* 2011;**378**:31–40
3. Dorenkamp M, Riad A, Stiehl S, Spillmann F, Westermann D, Du J, Pauschinger M, Noutsias M, Adams V, Schultheiss HP, Tschope C. Protection against oxidative stress in diabetic rats: role of angiotensin AT(1) receptor and beta 1-adrenoceptor antagonism. *Eur J Pharmacol* 2005;**520**:179–87
4. Westermann D, Van Linthout S, Dhayat S, Dhayat N, Schmidt A, Noutsias M, Song XY, Spillmann F, Riad A, Schultheiss HP, Tschope C. Tumor necrosis factor-alpha antagonism protects from myocardial inflammation and fibrosis in experimental diabetic cardiomyopathy. *Basic Res Cardiol* 2007;**102**:500–7
5. Pan Y, Wang Y, Zhao Y, Peng K, Li W, Wang Y, Zhang J, Zhou S, Liu Q, Li X, Cai L, Liang G. Inhibition of JNK phosphorylation by a novel curcumin analog prevents high glucose-induced inflammation and apoptosis in cardiomyocytes and the development of diabetic cardiomyopathy. *Diabetes* 2014;**63**:3497–511
6. Tsai KH, Wang WJ, Lin CW, Pai P, Lai TY, Tsai CY, Kuo WW. NADPH oxidase-derived superoxide anion-induced apoptosis is mediated via the JNK-dependent activation of NF-kappaB in cardiomyocytes exposed to high glucose. *J Cell Physiol* 2012;**227**:1347–57
7. Nizamutdinova IT, Guleria RS, Singh AB, Kendall JJ, Baker KM, Pan J. Retinoic acid protects cardiomyocytes from high glucose-induced apoptosis through inhibition of NF-kappaB signaling pathway. *J Cell Physiol* 2013;**228**:380–92
8. Zuo G, Ren X, Qian X, Ye P, Luo J, Gao X, Zhang J, Chen S. Inhibition of JNK and p38 MAPK-mediated inflammation and apoptosis by ivabradine improves cardiac function in streptozotocin-induced diabetic cardiomyopathy. *J Cell Physiol* 2019;**234**:1925–36
9. Malek V, Gaikwad AB. Telmisartan and thiorphan combination treatment attenuates fibrosis and apoptosis in preventing diabetic cardiomyopathy. *Cardiovasc Res* 2019;**115**:373–84
10. Suematsu Y, Miura S, Goto M, Matsuo Y, Arimura T, Kuwano T, Imaizumi S, Iwata A, Yahiro E, Saku K. LCZ696, an angiotensin receptor-neprilysin inhibitor, improves cardiac function with the attenuation of fibrosis in heart failure with reduced ejection fraction in streptozotocin-induced diabetic mice. *Eur J Heart Fail* 2016;**18**:386–93
11. Jaffuel D, Molinari N, Berdague P, Pathak A, Galinier M, Dupuis M, Ricci JE, Mallet JP, Bourdin A, Roubille F. Impact of sacubitril-valsartan combination in patients with chronic heart failure and sleep apnoea syndrome: the ENTRESTO-SAS study design. *ESC Heart Fail* 2018;**5**:222–30
12. Dec GW. LCZ696 (sacubitril/valsartan): can we predict who will benefit? *J Am Coll Cardiol* 2015;**66**:2072–4
13. Solomon SD, Zile M, Pieske B, Voors A, Shah A, Kraigher-Krainer E, Shi V, Bransford T, Takeuchi M, Gong J, Lefkowitz M, Packer M, McMurray JJ. The angiotensin receptor neprilysin inhibitor LCZ696 in heart failure with preserved ejection fraction: a phase 2 double-blind randomised controlled trial. *Lancet* 2012;**380**:1387–95
14. Ren XM, Zuo GF, Wu W, Luo J, Ye P, Chen SL, Hu ZY. Atorvastatin alleviates experimental diabetic cardiomyopathy by regulating the GSK-3beta-PP2Ac-NF-kappaB signaling axis. *PLoS One* 2016;**11**:e166740
15. Behr TM, Nerurkar SS, Nelson AH, Coatney RW, Woods TN, Sulpizio A, Chandra S, Brooks DP, Kumar S, Lee JC, Ohlstein EH, Angermann CE, Adams JL, Sisko J, Sackner-Bernstein JD, Willette RN. Hypertensive end-organ damage and premature mortality are p38 mitogen-activated protein kinase-dependent in a rat model of cardiac hypertrophy and dysfunction. *Circulation* 2001;**104**:1292–8
16. Liang Q, Bueno OF, Wilkins BJ, Kuan CY, Xia Y, Molkentin JD. c-Jun N-terminal kinases (JNK) antagonize cardiac growth through cross-talk with calcineurin-NFAT signaling. *EMBO J* 2003;**22**:5079–89
17. Khullar M, Al-Shudiefat AA, Ludke A, Binepal G, Singal PK. Oxidative stress: a key contributor to diabetic cardiomyopathy. *Can J Physiol Pharmacol* 2010;**88**:233–40

18. Hamid T, Guo SZ, Kingery JR, Xiang X, Dawn B, Prabhu SD. Cardiomyocyte NF-kappaB p65 promotes adverse remodelling, apoptosis, and endoplasmic reticulum stress in heart failure. *Cardiovasc Res* 2011;**89**:129–38
19. Yin H, Chao L, Chao J. Nitric oxide mediates cardiac protection of tissue kallikrein by reducing inflammation and ventricular remodeling after myocardial ischemia/reperfusion. *Life Sci* 2008;**82**:156–65
20. Mukhopadhyay P, Rajesh M, Horvath B, Batkai S, Park O, Tanchian G, Gao RY, Patel V, Wink DA, Liaudet L, Hasko G, Mechoulam R, Pacher P. Cannabidiol protects against hepatic ischemia/reperfusion injury by attenuating inflammatory signaling and response, oxidative/nitrative stress, and cell death. *Free Radic Biol Med* 2011;**50**:1368–81
21. Lee Y, Fluckey JD, Chakraborty S, Muthuchamy M. Hyperglycemia- and hyperinsulinemia-induced insulin resistance causes alterations in cellular bioenergetics and activation of inflammatory signaling in lymphatic muscle. *FASEB J* 2017;**31**:2744–59
22. Voors AA, Dorhout B, van der Meer P. The potential role of valsartan + AHU377 (LCZ696) in the treatment of heart failure. *Exp Opin Investig Drugs* 2013;**22**:1041–7
23. Suematsu Y, Jing W, Nunes A, Kashyap ML, Khazaeli M, Vaziri ND, Moradi H. LCZ696 (Sacubitril/Valsartan), an angiotensin-receptor neprilysin inhibitor, attenuates cardiac hypertrophy, fibrosis, and vasculopathy in a rat model of chronic kidney disease. *J Cardiac Fail* 2018;**24**:266–75
24. Qin W, Du N, Zhang L, Wu X, Hu Y, Li X, Shen N, Li Y, Yang B, Xu C, Fang Z, Lu Y, Zhang Y, Du Z. Genistein alleviates pressure overload-induced cardiac dysfunction and interstitial fibrosis in mice. *Br J Pharmacol* 2015;**172**:5559–72

(Received February 26, 2019, Accepted June 12, 2019)